Cancer Research

A Modeling Approach to Explain Mutually Exclusive and Co-Occurring Genetic Alterations in Bladder Tumorigenesis

Elisabeth Remy[1], Sandra Rebouissou[2,3], Claudine Chaouiya[4], Andrei Zinovyev[2,5,6], François Radvanyi[2,3], and Laurence Calzone[2,5,6]

Abstract

Relationships between genetic alterations, such as co-occurrence or mutual exclusivity, are often observed in cancer, where their understanding may provide new insights into etiology and clinical management. In this study, we combined statistical analyses and computational modeling to explain patterns of genetic alterations seen in 178 patients with bladder tumors (either muscle-invasive or non–muscle-invasive). A statistical analysis on frequently altered genes identified pair associations, including co-occurrence or mutual exclusivity. Focusing on genetic alterations of protein-coding genes involved in growth factor receptor signaling, cell cycle, and apoptosis entry, we complemented this analysis with a literature search to focus on nine pairs of genetic alterations of our dataset, with subsequent verification in three other datasets available publicly. To understand the reasons and contexts of these patterns of associations while accounting for the dynamics of associated signaling pathways, we built a logical model. This model was validated first on published mutant mice data, then used to study patterns and to draw conclusions on counter-intuitive observations, allowing one to formulate predictions about conditions where combining genetic alterations benefits tumorigenesis. For example, while *CDKN2A* homozygous deletions occur in a context of *FGFR3*-activating mutations, our model suggests that additional *PIK3CA* mutation or *p21CIP* deletion would greatly favor invasiveness. Furthermore, the model sheds light on the temporal orders of gene alterations, for example, showing how mutual exclusivity of *FGFR3* and *TP53* mutations is interpretable if *FGFR3* is mutated first. Overall, our work shows how to predict combinations of the major gene alterations leading to invasiveness through two main progression pathways in bladder cancer. *Cancer Res; 75(19); 4042–52. ©2015 AACR.*

Major Findings

Statistical analyses of bladder cancer genetic data reveal co-occurring or mutually exclusive genetic alterations for genes frequently altered in this cancer. The interactions between these genes are organized into an influence network based on literature analysis. We find that the sole network topology is not sufficient to explain some of the nine identified associations. To assess these associations while accounting for the dynamics of associated signaling pathways, we have developed a logical model. For the identified patterns, our model sheds light on aberrant activation of signaling pathways and provides predictions.

Introduction

Accumulated data show specific patterns of genetic and epigenetic changes associated with each cancer type. These patterns include particular sets of altered genes, types (mutations, amplifications, losses) and relationships (mutual exclusivity or co-occurrence) between alterations. The underlying molecular network should, at least partly, explain such observations. So far, these patterns have been explained in terms of linear pathways: co-occurring mutations tend to target genes in parallel signaling pathways, whereas mutual exclusive alterations may implicate genes involved either in a common pathway, or in different progression pathways, i.e., in different tumor types (1–5). Mutual exclusivity could also involve genes that are synthetically lethal (6). These explanations are only hand waving arguments, though. Indeed, the static network structure-based analysis of these patterns has its limitations. Pathways involved in tumorigenesis are complex and interconnected, and it is therefore difficult to define the borders of a signaling pathway, and the notion of parallel or common pathways. Mathematical modeling may help to go further in these interpretations.

[1]Aix Marseille Université, CNRS, Centrale Marseille, Marseille, France. [2]Institut Curie, PSL Research University, Paris, France. [3]CNRS, UMR 144, Oncologie Moléculaire, Equipe Labellisée Ligue Contre le Cancer, Institut Curie, Paris, France. [4]Instituto Gulbenkian de Ciência, Oeiras, Portugal. [5]INSERM, U900, Paris, France. [6]Ecole des Mines ParisTech, Fontainebleau, France.

Note: Supplementary data for this article are available at Cancer Research Online (http://cancerres.aacrjournals.org/).

Current addresses for S. Rebouissou: Inserm, UMR-1162, "Génomique Fonctionnelle des tumeurs solides," F-75010, Paris, France; Université Paris Descartes, Sorbonne Paris Cité, "Labex Immuno-Oncology," F-75000, Paris, France; Université Paris Diderot, Sorbonne Paris Cité, Institut Universitaire d'Hématologie, Paris, F-75010, France; Université Paris 13, Sorbonne Paris Cité, "Equipe Labellisée Ligue Contre le Cancer," F-93206 Saint-Denis, France.

E. Remy and S. Rebouissou contributed equally to this article.

Corresponding Author: Laurence Calzone, Institut Curie, PSL Research University, 75248 cedex 05 Paris, France. Phone: 3301-5624-6924; Fax: 3301-5624-6911; E-mail: laurence.calzone@curie.fr.

doi: 10.1158/0008-5472.CAN-15-0602

Quick Guide to Equations and Assumptions

Influence network

In an influence network, details of synthesis, degradation, phosphorylation, acetylation, or ubiquitination are abstracted into binary relations. Nodes (biochemical species or phenomena) are connected through directed, signed edges (denoting regulatory interactions). For instance, RB1 is known to sequester E2F1 by forming an inactive complex. This reaction is interpreted as RB1 inhibiting E2F1. Another example is the phenomenological node Proliferation, which is activated by both CyclinE1 and CyclinA. Throughout the article, when referring to the genes, their names will be italicized (e.g., *CCND1*), and the nodes of the network will be written in standard format (e.g., CyclinD1).

Dynamical, logical model

From the influence network, we define a discrete, dynamical model using the logical formalism. Our qualitative representation of genomic data (mutation, loss, or amplification of a gene locus) justifies a discrete modeling approach. Each node of the network is associated with a discrete variable representing its qualitative functional level. A Boolean variable is often sufficient to convey the role of the corresponding node: species are either active (ON) or inactive (OFF), thus able, or not, to act upon their targets. In some cases, more than two levels are needed to convey distinct functional roles. For instance, E2F1 mediates the transcription of cell-cycle genes, but when overexpressed, it activates genes of the apoptotic pathway. To distinguish between these two situations, E2F1 is associated with a multivalued variable (values 0, 1, or 2).

The variables describe the current node states, which evolve depending on logical rules. More precisely, the target level of each node is defined by a set of logical statements on the levels of the regulators of that node using logical connectors (denoted ! for NOT, & for AND, and | for OR).

For example, the Boolean variable associated with Proliferation evolves as follows:

$$\text{Proliferation} = 1\text{IF}\,(\text{CyclinE1} \mid \text{CyclinA}) \tag{A}$$

Statement (1) indicates that Proliferation is ON if one of the cyclins is present (otherwise *Proliferation* is OFF). The case of the multivalued variable associated with E2F3 (which stands for the isoform E2F3a) is more complex. Its logical rule includes one logical formula for each level:

$$\text{E2F3} = 1\text{IF}\,(!\text{RB1}\ \&!\text{CHEK1\_2}:2\ \&\text{RAS}) \tag{B}$$

$$\text{E2F3} = 2\text{IF}\,(!\text{RB1}\ \&\,\text{CHEK1\_2}:2\ \&\text{RAS}) \tag{C}$$

Statement (2) specifies under which conditions the target level of E2F3 is 1: simultaneous absence of RB1 (inhibitor of E2F3), of CHEK1_2 (which stands for either CHEK1 or CHEK2) at its maximum value, and presence of RAS. Statement (3) specifies under which conditions E2F3 level is 2: E2F3a is induced by DNA damage in a CHEK1/2-dependent manner in the absence of RB1 and in the presence of RAS. For any other situation, the target value of E2F3 is 0.

Given a state of the model, that is, a vector of all node levels, some of the nodes may be called to update their levels as prescribed by their logical rules. Because we have no information about the velocities of these changes, we opt for the asynchronous update that defines as many successor states as the number of updated nodes. The resulting discrete dynamics is nondeterministic (a state may have several successors) and covers all potential behaviours of the network, compatible with the logical rules.

The attractors of the logical model refer to long-term behaviors (sets of states in which the dynamics is trapped). These attractors are stable states (all nodes are stable) or complex attractors (some nodes display oscillations).

In this modeling framework, perturbations of gene activity are defined as follows: variable associated with the perturbed node is constrained, overriding its logical rule. A gain of function, amplification, or overexpression is specified by maintaining a variable at 1 (or at its maximal level in the case of a multivalued variable), and is denoted by the broad term "overexpression," whereas a loss of function or deletion is defined by maintaining a variable at 0 (denoted KO).

Assessing phenotypes

To interpret the model results, we associate observed biologic phenotypes with attractors of the discrete model. These attractors correspond to phenotypes specified by the states of the output nodes: Proliferation, Apoptosis (E2F1 or TP53-dependent), and Growth_arrest. From a given set of initial conditions, the possible fates of a cell are assessed in terms of the phenotypes that can be reached from these conditions and the probabilities associated to those phenotypes. Associating a phenotype with a stable state is straightforward, whereas a cyclic attractor may include oscillations between several phenotypes when the cell decision cannot be made. The probability of a phenotype is estimated as the proportion of trajectories leading to any attractor matching this phenotype. Input components are maintained constant (corresponding to external signals). While some input values lead to multistability (several possible phenotypes), some others drive the cell, deterministically, to a unique phenotype; for example, in most cases, the sole Apoptosis is possible when DNA_damage is ON.

Here, we show how dynamical modeling can relate complex networks with observable biologic data (genomic alterations, mutations). Computational modeling allows to integrate and validate current knowledge about molecular mechanisms underlying cellular decisions. It supports mechanistic understanding and helps to formulate predictions when the network complexity defies intuition. This is particularly true when dealing with diseases such as cancer, which involve the deregulation of multiple and intricate pathways (7). Numbers of models have already proved useful in elucidating questions related to cancer biology (8–13).

Bladder cancer is frequent in Europe and North America, where it represents the fourth most common cancer in men and the ninth in women in terms of incidence (14). The high recurrence rate makes bladder cancer one of the most costly cancers to treat. Many observations of the patterns of genetic changes identified in bladder cancer studies remain unexplained or only partially explained in terms of underlying molecular mechanisms (15, 16). Bladder tumors progress along two main pathways: Ta and CIS (carcinoma *in situ*) pathways (17, 18). About 50% of diagnosed bladder carcinomas are Ta tumors, generally of low grade; 20% are T1 tumors and 30% are muscle-invasive tumors (T2–4). CIS consists of flat, high-grade lesions, rarely found in absence of other bladder tumors. Ta tumors often recur and progress rarely (5 to 10% of cases) but unpredictably to T1 and then to muscle-invasive tumors (T2–4), whereas CIS often progress to T1 and then to muscle-invasive tumors *in circa* 50% of the cases. It is believed that about 80% of muscle-invasive tumors develop through the CIS pathway. In bladder cancer, as in many cancer types, an important fraction of genetic alterations concerns genes coding for growth signaling factors and for G1–S regulators. Activating mutations of the fibroblast growth factor receptor 3 (*FGFR3*) gene are associated with the Ta pathway with a high frequency, but are rarely found in the CIS pathway (17). Besides *FGFR3*, mutated in about 45% of tumors (19), common genes recurrently genetically altered include other oncogenes such as the small GTPases *HRAS* (9% of cases) and *KRAS* (4% of cases), *PIK3CA* (subunit of the PI3K, 18% of cases), as well as tumor suppressors such as *CDKN2A* (16% of cases) and *RB1* (20% of cases; ref. 52). Mutations affecting oncogenes are recurrent point mutations, whereas *CDKN2A* is mostly affected by losses involving the whole gene (20). *RB1* is targeted by both point mutations and deletions (21).

Our goal is to understand how genetic alterations (mutations, homozygous deletions, or amplifications) combine to promote cancer tumorigenesis. More precisely, we aim to explore patterns (mutual exclusivity or co-occurrence), focusing on components often altered in bladder cancer and involved in growth factor signaling, cell-cycle entry, and triggering of apoptosis in response to DNA damage with the focus on the E2F pathway. It has been shown recently that the E2F pathway is not only involved in the control of proliferation but also in invasion and metastasis (22–24), justifying the study of this pathway to explore invasiveness in bladder tumors.

This study combines literature search, statistical analysis of relevant datasets and logical modeling of the related signaling network. Using an initial dataset of 178 tumors (CIT series) and three public datasets, statistical tests on pairs of alterations identify a list of co-occurring or mutually exclusive alterations. With our computational model, we analyze each association to identify the deregulated pathways and their contribution to tumorigenesis. In some cases (e.g., co-occurrence of *FGFR3* and *PIK3CA* mutations), we found that the sole network topology cannot explain the alteration patterns identified by statistical analysis. It appears necessary to build a dynamical model to accurately and formally identify mechanisms activated in these patterns (25). When the model cannot straightforwardly account for these patterns, we search for contexts (other activating or inactivating mutations, amplifications or losses) that could explain the statistical results. Mathematical modeling provides insights into properties of involved cellular pathways. It is thus useful to understand mechanisms at play, as a complement to statistical methods, which uncover patterns of alterations. Here, our main goal is to highlight mechanisms affected in bladder tumors to propose successive events that may lead to high-stage tumors in both Ta and CIS progression pathways.

Materials and Methods

Data production and analysis

Bladder samples (CIT series). One hundred seventy-eight bladder carcinomas, including 90 non–muscle-invasive tumors (50 pTa, 40 pT1) and 88 muscle-invasive tumors (32 pT2, 37 pT3, 19 pT4), were collected from patients treated surgically between 1988 and 2006 at Henri Mondor Hospital (Créteil, France), Institut Gustave Roussy (Villejuif, France) and Foch Hospital (Suresnes, France). All tumors were pathologically reviewed, staged according to the 2002 TNM classification (26, 27), and graded according to the 1973 WHO classification (28). All patients provided written informed consent, and ethics committees of all hospitals approved the study (Comité de Protection des Personnes de l'hôpital Henri Mondor, Comité de Protection des Personnes de Boulogne—Ambroise Paré, and Comité de Protection des Personnes de Bicêtre). All analyses were performed on the basis of anonymous patient data.

DNA extraction from tissues. Immediately after surgery, tissue samples were frozen in liquid nitrogen and stored at −80°C until nucleic acid extraction. DNA were extracted from frozen human bladder tissues as described in (26).

Gene mutation analysis. *FGFR3* mutations were studied with the SNaPshot method (29). *TP53* (exons 2–11), *KRAS* (exons 2–3), *NRAS* (exons 2–3), *HRAS* (exons 2–3) and *PIK3CA* (exons 2, 9, and 20) gene mutations were screened by direct sequencing with previously described primers and protocols (30, 31), available on request. All mutations were confirmed by sequencing both strands of a second, independent PCR product.

CGH array analysis. DNA copy number was analysed for the 178 bladder tumors on the human genome-wide CIT-CGH array (V6) designed by the CIT-CGH Consortium. This array contains 4,434 sequence-verified bacterial artificial chromosome (BAC) and P1-derived artificial chromosome (PAC) clones. Genomic alterations were determined using GLAD algorithm (32).

Multiplex ligation-dependent probe amplification analysis. DNA copy number at the *CDKN2A* and *RB1* loci was determined using a MLPA assay, as described in ref. 33. Bladder tumor DNA was analyzed with the P024B kit and P047 kits (MRC-Holland, Amsterdam, the Netherlands) for genomic analysis of *CDKN2A/B* and *RB1*, respectively. Two of the 14 control probes

Table 1. Table of associations of pairs of alterations (first column) identified in the literature (2nd column), in CIT dataset (3rd to 5th columns), and verified in public datasets (from 6th to 11th columns: Lindgren, Iyer, TCGA datasets, and all invasive from Lindgren, Iyer and TCGA)

			Observed in data											
	Associations	Reported in the literature	CIT	CIT sup	CIT inv	Lindgren	Lindgren sup	Lindgren inv	Iyer	TCGA	Invasive (public data)	Explained by the model	Model predictions
1													
1.1	Mutual exclusivity *FGFR3* mut–*RAS* mut	Yes	**0.009**	**0.002**	1	0.235	**0.088**	NA	1	0.604	0.22	Yes	
1.2	Mutual exclusivity *FGFR3* mut–*E2F3* ampl	No	**0.017**	**0.078**	1	**0.041**	**0.035**	0.159	**0.067**	0.195	**0.001**	Yes	
1.3	Mutual exclusivity *FGFR3* mut–*CCND1* ampl	No	**0.009**	**0.005**	1	1	0.592	0.23	0.21	1	0.619	No	Yes
1.4	Co-occurrence *FGFR3* mut–*PIK3CA* mut	Yes	**0.0231**	0.177	0.11	**0.035**	0.379	0.131	1	0.764	1	Yes, but only in a particular context	Yes[a]
2													
2.1	Co-occurrence *FGFR3* mut–*CDKN2A* homozygous del	Yes (in invasive tumors)	**0.039**	0.569	**0.0013**	1	0.495	0.126	**0.011**	**0.009**	**0.0002**	Yes, but only in a particular context	Yes[a]
2.2	Mutual exclusivity *FGFR3* mut–*TP53* mut	Yes (when considering all tumors only)	**0.0006**	0.226	1	**0.005**	0.114	0.41	**0.033**	0.32	**0.039**	Difficult to conclude	Yes
3	Co-occurrence *TP53* mut–*E2F3* ampl	No	**0.0007**	**0.059**	**0.058**	**0.099**	**0.005**	0.677	**1E-05**	0.493	**0.0026**	Yes	Yes
4													
4.1	Co-occurrence *CDKN2A* homozygous del–*CCND1* ampl	No (but found in head and neck tumors)	**0.043**	**0.006**	1	0.3	0.39	0.56	**0.072**	0.78	0.7	Yes	
4.2	Co-occurrence *CDKN2A* homozygous del–*PIK3CA* mut	No	**0.044**	0.67	**0.011**	**0.033**	0.68	**0.003**	1	0.243	0.7	Yes	
col	1	2	3	4	5	6	7	8	9	10	11	12	13

NOTE: Co-occurrence and exclusivity patterns are confronted to the model (12th column); predictions are proposed (13th column).

[a]Verification was impossible in other datasets because of the limited amount of samples. The *P* values of the Fisher exact tests are reported in bold, significant *P* values (<0.1).

spanning chromosomal regions 9q21 and 11p12 were excluded from the *RB1* copy number analysis because these regions are frequently altered in bladder tumors.

Testing mutual exclusivity and co-occurrence of genetic alterations. Table 1 reports *P* values of the Fisher exact tests for all pairs of selected genetic alterations. For each alteration, we split the tumor samples into two groups with and without the alteration, and analyzed the corresponding contingency tables for pairs of alterations. The significance threshold was set to 5%. We performed the tests using R software.

Computational network modeling. The modeling framework is presented in the Quick Guide to Equations and Assumptions. Model construction and analysis were done with GINsim software (34); probabilities for wild-type and mutant phenotypes were calculated using Avatar (35) and MaBoSS (36).

Results

Figure 1 depicts the workflow designed for this study. We first searched the literature on published co-occurrence and mutual exclusivity patterns, focusing on genetic alterations (mutations, homozygous losses, and amplifications) of genes known to be frequently altered in bladder cancer and reported in previous studies (37, 38). These genes code mainly for proteins involved in growth factor receptor signaling (*EGFR*, *FGFR3*, *HRAS*/*KRAS*/*NRAS*, *PIK3CA*), cell-cycle entry (*RB1*, *RBL2*, *CDKN2A*, *CCND1*, *E2F3*), and in triggering apoptosis in response to DNA damage (*TP53*, *MDM2*; Fig. 2B; Supplementary Material S1). Among the selected genes, we performed a statistical analysis on our dataset, referred to as CIT dataset, including 178 samples of bladder carcinomas, with non–muscle-invasive and muscle-invasive tumors (Fig. 2A; Supplementary Table S9). We finally verified the patterns deduced from both the literature search and the statistical analysis in three additional independent bladder tumor datasets [referred to as the Lindgren dataset (37), the Iyer dataset (38), and the TCGA dataset (39)].

A model including the selected genes was built using molecular facts extracted from scientific publications. It was validated against published phenotypes of mice mutants (Supplementary Table S3). Both the topological analysis of the network and the mathematical model were used to explain the patterns of alterations, formulate predictions such as expected effect of genetic contexts, or yet probe results from the data analysis. When possible, model predictions were verified in the datasets.

Data analysis of patterns of co-occurrence and mutual exclusivity

The identified associations concern: *FGFR3*, *RAS*, *PIK3CA*, *CCND1*, *E2F3* (oncogenes) and *RB1*, *TP53*, *CDKN2A* (tumor suppressors). We organized these associations into four groups (Table 1): (1) mutual exclusivity or co-occurrence of *FGFR3* mutations and genetic alterations of another oncogene; (2) co-occurrence or mutual exclusivity of *FGFR3* mutations and alterations of tumor suppressors; (3) co-occurrence of *TP53* mutations and *E2F3* amplifications; and (4) co-occurrence of *CDKN2A* homozygous deletions and oncogenes besides *FGFR3*.

We found associations between genetic alterations in the literature (Table 1, column 2): exclusivity of *FGFR3* and *RAS*-activating mutations (Table 1; row 1.1; ref. 16); co-occurrence of

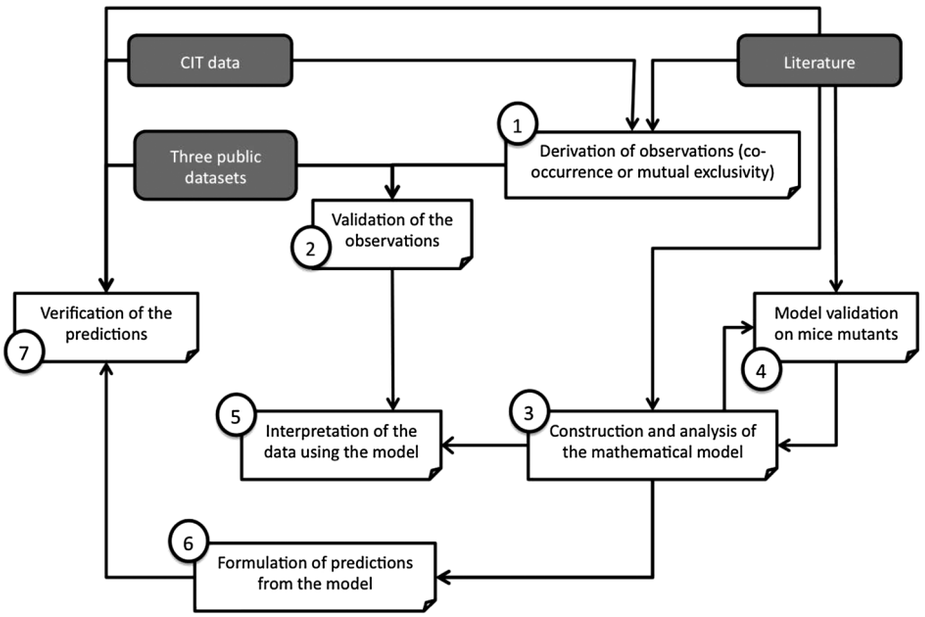

Figure 1.
Flowchart of our study to explain patterns of genetic alterations. Gray boxes denote data sources while folded corner rectangles denote the seven steps of our workflow, in the sequence indicated by the tokens. Gray boxes concern data. White boxes include statistical analyses or computational modeling.

FGFR3 and *PIK3CA*-activating mutations (Table 1; row 1.4; refs. 15, 40); co-occurrence of *FGFR3* mutations and *CDKN2A* homozygous deletions in muscle-invasive tumors (Table 1, row 2.1; ref. 33); exclusivity of *FGFR3* and *TP53* mutations, found when considering all tumors but disappearing when stratifying by stage (Table 1, row 2.2; ref. 19); and co-occurrence of *E2F3* amplifications and *RB1* deletions (or *CDKN2A* deletions as presented in ref. 41).

On CIT dataset, we performed the Fisher exact test of independence for each pair of alterations (Table 1, columns 3–5). Because some associations depend on the stage, we considered all tumors and separately: non–muscle-invasive (sup) and muscle-invasive tumours (inv). Note that stratifying tumors by both stage and grade would have resulted in subgroups too small to achieve statistically significant tests. We found associations not previously reported in the literature for bladder cancer: exclusivity of *FGFR3* mutations and *E2F3* amplifications (Table 1, row 1.2); exclusivity of *FGFR3* mutations and *CCND1* amplifications (Table 1, row 1.3); co-occurrence of *TP53* mutations and *E2F3* amplifications (Table 1, row 3); co-occurrence of *CCND1* amplifications and *CDKN2A* homozygous deletions (Table 1, row 4.1, reported in other cancer types; refs. 42, 43); and co-occurrence of *PIK3CA* mutations and *CDKN2A* deletions (Table 1, row 4.2).

Proceeding with our workflow, we mined three publicly available datasets, searching for associations found in the literature and/or in our CIT dataset. We considered each dataset separately

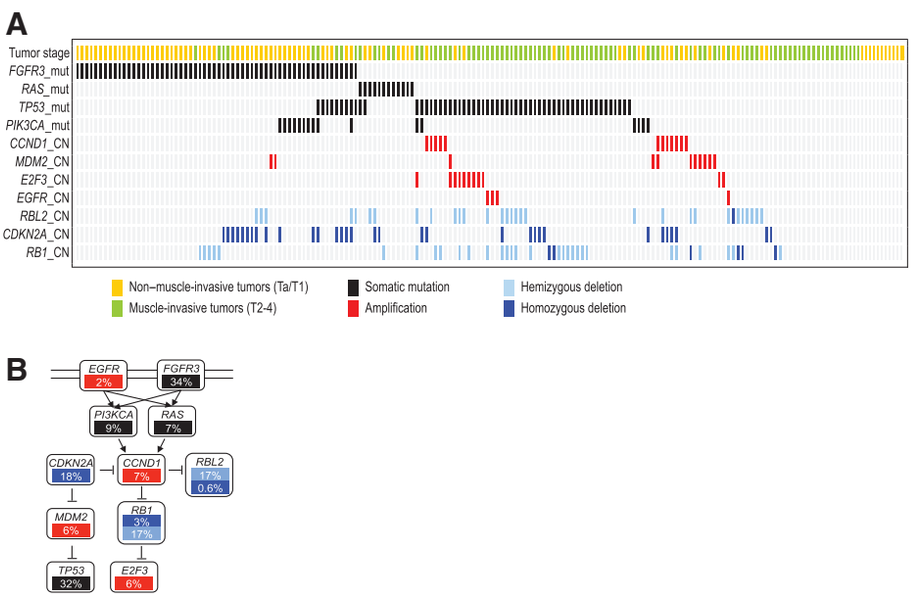

Figure 2.
Overview of genes frequently altered in bladder cancer. A, mutations and copy number alterations for 11 genes are shown for each tumor of the CIT dataset. B, pathways involving these 11 genes: percentage of each alteration identified in the CIT dataset is indicated; black, somatic mutations; blue, homozygous deletions; red, amplifications of genes. Edges between genes represent known influences; normal arrows, positive effects; blunt arrows, negative effects.

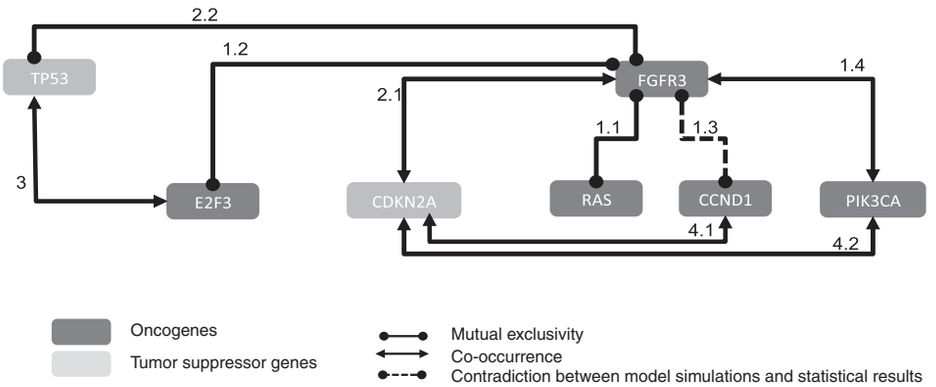

Figure 3.
Representation of the statistical results for co-occurrence and mutual exclusivity patterns. Arrow labels correspond to association number of Tables 1 and 2. Dashed association between FGFR3 and CCND1 (1.3) denotes a contradiction between model simulations and statistical analysis.

(Table 1, columns 6–10), as well as an ensemble gathering all muscle-invasive datasets (Lindgren, Iyer, and TCGA muscle-invasive tumors; Table 1, column 11). Non–muscle-invasive tumors, besides the CIT dataset, are only found in the Lindgren dataset. Among the published associations, all were confirmed in at least one of the four datasets, except for the last one: co-occurrence of *E2F3* amplifications and *RB1* deletions was not found significant in any dataset (not shown). We thus chose not to further study it. Eight out of these nine remaining patterns were verified in at least one of the three public datasets (Table 1, rows 1.1 and 4.1). Figure 3 recapitulates these associations.

Computational network modeling

From the influence network to the logical model. On the basis of an extensive literature search and on our previous work (44), we built a generic simplified influence network around E2F-activating transcription factors in response to cell receptor activation (EGFR and FGFR3), growth inhibition (mainly representing TGFβ) and DNA damage, yet focusing on genes altered in bladder cancer. We considered the major players involved in both RB/E2F and TP53 pathways, controlled by the same transcription factor, E2F1, which included the genes identified in the data analysis.

The network of Fig. 4 summarizes information from the literature and from pathway databases, such as Reactome (45) or Atlas of Cancer Signaling Network (53). It includes 30 nodes and 84 interactions. The inputs, DNA_damage, EGFR_stimulus, FGFR3_stimulus and Growth_inhibitors, trigger different responses (also referred to as phenotypes): Apoptosis, Proliferation, and Growth_arrest. Readouts for these phenotypes are: presence of CyclinE1 (*CCNE1*) or CyclinA (*CCNA2*) for proliferation, of TP53 for E2F1-independent apoptosis, of E2F1 for E2F1-dependent apoptosis, and of p21CIP (*CDKN1A*), RBL2 or RB1 for growth arrest. These molecular readouts are considered as phenotype triggers, possibly followed by downstream events, not described here. For example, when either CyclinE1 or CyclinA is

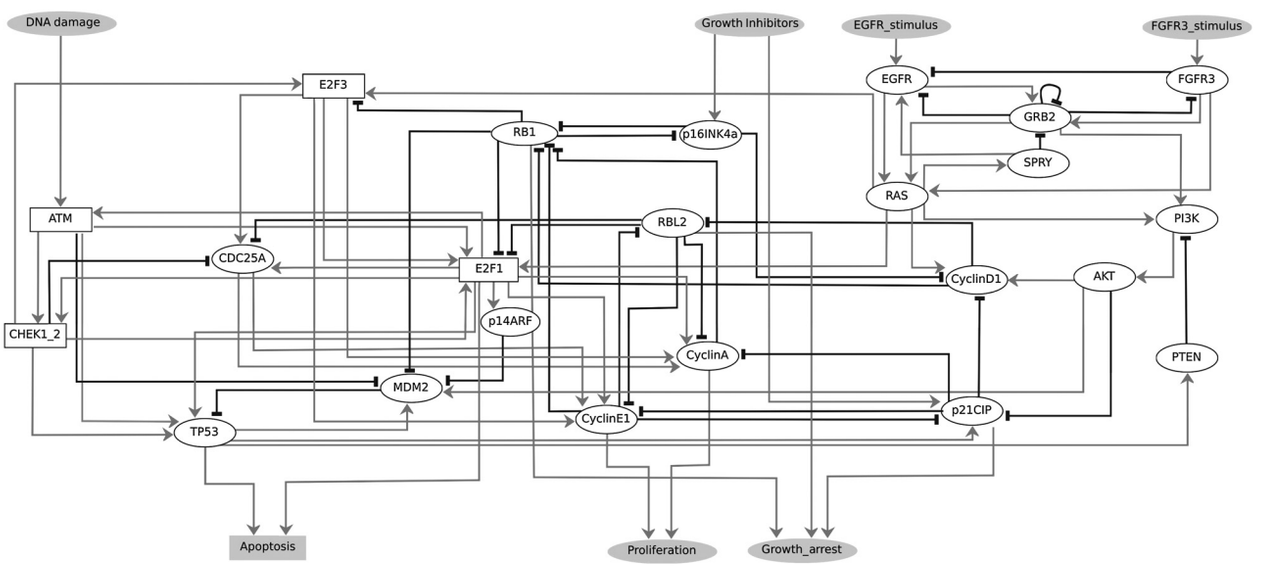

Figure 4.
Influence network of the species involved in entry into apoptosis and cell cycle, through E2F1. Nodes denote species or phenotypes; edges denote influences. Gray arrows, positive influences; T-shaped arrows, negative influences. Rectangular nodes depict multivalued variables and ellipsoid nodes Boolean variables. Input and output nodes are in gray.

active, it indicates that the cell enters S-phase. Similarly, TP53 activation does not necessarily lead to apoptosis but rather triggers it (Supplementary Material S1).

Growth factors are separated into two stimuli, EGFR_stimulus and FGFR3_stimulus, the first activating EGF receptor (EGFR), and the second activating FGFR3. Pathways downstream of the two receptors differ based on SPRY activity. This interplay between EGFR and FGFR3 has been abstracted from Grieco and colleagues (12).

From the influence network, we defined the logical model, with 25 Boolean variables and five ternary variables. Each combination of input values thus defines a region of the state space with over 10^9 states. The logical rules governing model dynamics (see Quick Guide to Equations and Assumptions) are described in Supplementary Table S1. The model has 20 stable states and 5 cyclic attractors (Supplementary Table S2). These attractors correspond to phenotypes described by the values of Apoptosis, Proliferation, and Growth_arrest. In some cases, the input combination fully determines the resulting phenotype: for DNA_damage ON, there is a unique attractor where Apoptosis and Growth_arrest are ON and, conversely, this phenotype is only possible in the presence of DNA_damage. Some input values lead to two stable states (multistability): for DNA_damage OFF, FGFR3_stimulus and Growth_inhibitors ON, either Proliferation or Growth_arrest is possible. Some complex attractors show oscillations between two of the phenotypes: for EGFR_stimulus ON and the other inputs OFF, oscillations between Growth_arrest and Proliferation are observed.

To test the model coherence, we challenged it with published experiments on diverse cell types (mouse embryo and rat fibroblasts, murine retina, etc.) by targeting the corresponding network nodes, and checking that our model qualitatively reproduces mutant phenotypes (Supplementary Table S3).

Data interpretation using the model

In the light of the model properties, we verified the possible cooperating or exclusive mechanisms corresponding to associations. To support our findings, for each association, we considered the corresponding mutants and quantified the related phenotypes (Material and Methods, Table 1; Supplementary Fig. S1).

Mutual exclusivity between *FGFR3* and *RAS* mutations is confirmed by our model. As shown in the network (Fig. 4), FGFR3 is upstream of RAS (in our model, FGFR3 directly activates RAS). Hence, for FGFR3-overexpressed mutant, RAS is active in all stable states and, consequently, additional mutations of *RAS* do not alter these phenotypes; there is no advantage for the tumor to mutate *RAS* when *FGFR3* is already mutated. Note that single RAS-overexpressed mutant has a higher probability of Proliferation phenotype, which can also be reached through EGFR signaling (Table 2; Supplementary Fig. S1). In the case of single FGFR3 mutant, EGFR is always OFF (due to mutual inhibition of FGFR3 and EGFR through PKC; ref. 12), which implies that there are less trajectories leading to Proliferation. The model thus confirms the exclusivity of the two alterations: if *FGFR3* is mutated, there is no advantage to further mutate *RAS*. For the same reasons, we predict that *EGFR* amplifications and *RAS* mutations are mutually exclusive. This could not be verified in the datasets due to the low percentage of both genetic alterations (46).

Mutual exclusivity between *FGFR3* mutations and *E2F3* amplifications, not reported in the literature but suggested in the CIT dataset, is also found in the Lindgren dataset and in pooled muscle-invasive samples. Because *FGFR3* is upstream of *E2F3* (Fig. 4), we expect that the genes activated by *E2F3* are also activated by *FGFR3*. Indeed, the model shows that E2F3 is activated when FGFR3 activity is forced and simulations confirm that there is no advantage for the cancerous cell to amplify *E2F3* if *FGFR3* is already mutated (Table 2; Supplementary Fig. S1). Proliferation probability slightly decreases in the double mutant compared with single E2F3 overexpressed mutant for reasons similar to those evoked for the previous association.

Mutual exclusivity of *FGFR3* mutations and *CCND1* amplifications is suggested in CIT superficial tumors but has not been reported so far in the literature, and is not confirmed in other datasets. Our model shows an increase in proliferation when further amplifying *CCND1* in an *FGFR3*-mutated tumor (Table 2; Supplementary Fig. S1), thus contradicting the exclusivity observed in our CIT data but in agreement with absence of this pattern in other datasets. *CCND1* can be activated by *FGFR3*, but may have additional beneficial roles for the tumor, not explained by the model straightforwardly (dashed line in Fig. 3). Indeed, we find that in the single FGFR3 mutant (with DNA damage ON), the apoptotic phenotype is TP53-dependent, whereas it is also E2F1-dependent in the single CyclinD1 mutant. CyclinD1 presumably plays an additional role in triggering apoptosis by forcing E2F1 activation or inhibiting RBL2. The role of *CCND1* gene in bladder would require further investigation.

Co-occurrence of *FGFR3* and *PIK3CA* mutations is reported in the literature (15, 40) and found significant in the CIT and Lindgren datasets. As CyclinD1, PI3K is downstream of FGFR3 (Fig. 4). Consequently, when FGFR3 is active, so should be PI3K, which is not the case, because GRB2 is needed for PI3K activation. The sole interpretation of the network topology is thus not enough to explain the advantage to mutate both PI3K and FGFR3. To investigate this co-occurrence, we simulated the single mutants FGFR3-overexpressed or PI3K-overexpressed, and the double mutant FGFR3 PI3K overexpressed. From a qualitative point of view, no striking difference appears between the three mutants: the same phenotypes are reached, the only difference being the appearance of E2F1-dependent apoptosis in PI3K-overexpressed mutant (not shown) as previously observed with CyclinD1-overexpressed mutant. It seems advantageous in terms of Proliferation probabilities to mutate FGFR3 in PI3K-mutated tumours ("Null" phenotype corresponds to stable states with inputs all OFF, AKT pathway forced, and thus survival probably activated). From the single FGFR3-overexpressed to the double FGFR3 and PI3K-overexpressed mutant, only a slight increase in proliferation is observed (Table 2; Supplementary Fig. S1). We would expect *PI3K*-activating mutations to favor uncontrolled growth in an *FGFR3*-mutated context by promoting survival and blocking apoptosis. However, our model shows that it is not the case: to fully lead to uncontrolled proliferation, other checkpoints need to be deleted, for example, *CDKN2A*. The systematic analysis of multiple mutants predicts that indeed, a third deletion of *CDKN2A* (equivalent to p16INK4a KO in our simulations) abolishes all Growth_arrest stable states and thus, in absence of DNA damage, the sole reachable phenotype is Proliferation (Supplementary Tables S4–S7). We verified this observation in the data, but unfortunately, there are too few samples with the three alterations to perform significant statistical tests; however, among the 12 samples that carry the double mutations *FGFR3* and

Table 2. Effect of single and double mutations with respect to wild type for single mutants (Single_Mut/WT) and with respect to single mutants for double mutants (Double_Mut/Single_Mut)

	Mutants	Prolif	Apop	GA	P/GA	Null
1.1	FGFR3/WT	++	Same	−−	Disappear	Same
	RAS/WT	++	Same	−−	Disappear	Same
	Double mutant/FGFR3	Same	Same	Same	Same	Same
	Double mutant/RAS	−−	Same	++	Same	Same
1.2	FGFR3/WT	++	Same	−−	Disappear	Same
	E2F3/WT	++	Same	−−	Disappear	Same
	Double mutant/FGFR3	Same	Same	Same	Same	Same
	Double mutant/E2F3	−	Same	+	Same	Same
1.3	FGFR3/WT	++	Same	−−	Disappear	Same
	CyclinD1/WT	++	Same	−−	Same	++
	Double mutant/FGFR3	+	Same	Same	Same	Same
	Double mutant/CyclinDl	++	Same	+	Same	Disappear
1.4	FGFR3/WT	++	Same	−−	Disappear	Same
	PI3K/WT	++	Same	−−	Disappear	++
	Double mutant/FGFR3	+	Same	Same	Same	Same
	Double mutant/P13K	++	Same	−	Same	Disappear
2.1	FGFR3/WT	++	Same	−−	Disappear	Same
	CDKN2A/WT	+	Same	−−	++	Same
	Double mutant/FGFR3	+	Same	−	Same	Same
	Double mutant/CDKN2A	++	Same	−	Disappear	Same
2.2	FGFR3/WT	++	Same	−−	Disappear	Same
	TP53/WT	Same	−−	++	Same	Same
	Double mutant/FGFR3	Same	−−	++	Same	Same
	Double mutant/TP53	++	+	−−	Disappear	Same
3	TP53/WT	Same	−−	++	Same	Same
	E2F3/WT	++	Same	−−	Disappear	Same
	Double mutant/TP53	++	Same	−−	Disappear	Same
	Double mutant/E2F3	Same	−−	++	Same	Same
4.1	CDKN2A/WT	+	Same	−−	++	Same
	CyclinD1/WT	++	Same	−−	Same	++
	Double mutant/CDKN2A	++	Same	−−	−−	++
	Double mutant/CyclinD1	++	Same	−−	Same	Same
4.2	CDKN2A/WT	+	Same	−−	++	Same
	PI3K/WT	++	Same	−−	Disappear	++
	Double mutant/CDKN2A	++	Same	Disappear	Disappear	++
	Double mutant/PI3K	++	Same	Disappear	Same	++

NOTE: ++, increase higher than 10% (in absence of DNA damage); +, an increase higher than 5%; −−, decrease higher than 10% (in absence of DNA damage); −, a decrease higher than 5%.

PIK3CA, the two samples that are muscle-invasive have lost the two copies of *CDKN2A*.

Co-occurrence of *FGFR3* mutations and *CDKN2A* homozygous deletions has been documented; Rebouissou and colleagues (33) reports that *CDKN2A* (hemizygous and homozygous) losses predict progression of *FGFR3*-mutated tumors, and *CDKN2A* homozygous deletion is associated with muscle-invasive tumors; Lindgren and colleagues consider *CDKN2A* deletions as a late event in tumorigenesis in *FGFR3*-mutated tumors (data from 2010; ref. 37). This co-occurrence is found in the CIT dataset and confirmed in the Iyer and TCGA datasets, suggesting that it is indeed prevalent in muscle-invasive tumors. In our model, in an *FGFR3*-mutated context, loss of *CDKN2A* shows a slight increase in proliferation (Table 2; Supplementary Fig. S1), hence no clear advantage for co-occurrence of these two alterations. As mentioned above, mutations of *PIK3CA*, but also deletions of *CDKN1A* (*p21CIP*) would drastically favour proliferation (Supplementary Tables S4 and S8). Recall that RB/E2F pathway is not only involved in proliferation but also in invasion and metastasis (22–24); thus, we anticipate that highly proliferative tumors are invasive (Supplementary Fig. S2 shows that expression of gene targets of the E2F1-3 transcription factors is correlated to tumor stages). p21CIP seems to be a good candidate for progression toward invasiveness. This is supported by the reported association of *p21CIP* with poor clinical outcome in urothelial bladder cancer (47). Unfortunately, there are two few samples to achieve statistical significance for *p21CIP* alterations in the CIT or TCGA datasets, even though among the five tumors that are both *FGFR3*-mutated and *p21CIP*-altered in TCGA (i.e., mutated or deleted), four are *CDKN2A* homozygously deleted.

The model also suggests that the double mutant EGFR overexpressed and CDKN2A deleted (equivalent to *EGFR* amplifications and *CDKN2A* homozygous loss) gives similar results as the triple mutant FGFR3-mutated, PI3K-mutated, and CDKN2A deletion: only Proliferation phenotypes are reached in absence of DNA damage. In the CIT dataset, *EGFR*-amplified tumors (which belong to the basal-like bladder tumor subtype; ref. 48) do not seem to lose *CDKN2A* more frequently than *FGFR3*-mutated tumors, and, more surprisingly, *CDKN2A* expression is increased when compared with the nonbasal tumors. This suggests two things: (i) CDKN2A may compensate transcriptionally for the loss of RB activation in these tumors; and (ii) in bladder, FGFR3 activates the cell cycle through CDK4/6 (CDKN2A-dependent), whereas EGFR activates the cell cycle in a CDKN2A-independent

manner. In agreement with this idea, CCNB1 and CCNE2, whose actions are CDKN2A-independent, are both overexpressed in basal-like bladder tumors presenting an activation of EGFR target genes (48).

Mutual exclusivity of *FGFR3* and *TP53* mutations has been reported for all tumors rather than tumors separated by stage (19). In our model, when TP53 is mutated, Apoptosis is still reachable through E2F1, whereas Apoptosis is only TP53-dependent in FGFR3 single mutant (not shown). Model simulations indicate that TP53 mutations in an FGFR3-mutated context have little impact on proliferation (Table 2; Supplementary Fig. S1); however, mutating FGFR3 in a TP53-mutated context clearly increases Proliferation probability. The model shows that, when TP53 is already mutated, it is advantageous to mutate any gene from the cell-cycle machinery (here *FGFR3*, but amplification of any oncogene from our network would serve, as shown in the next association). From these results, we can only conclude that mutual exclusivity may concern *FGFR3*-mutated tumors.

We anticipate that *EGFR* amplifications and mutations of *TP53* would be associated in muscle-invasive tumors. In the data, the amplifications for *EGFR* are rare (4 in CIT, 1 in Lindgren, 0 in Iyer, 10 in TCGA). But, recently, a subgroup of tumors was identified with overexpression of *EGFR* (either through transcriptional mechanisms or amplification) and indeed enriched with *TP53* mutations (48).

Co-occurrence of *TP53* mutations and *E2F3* amplifications has not been reported but appears significant in CIT data. The model shows an increase in proliferation when comparing TP53 single mutant with the double mutant TP53-deleted E2F3-overexpressed, which is not the case when comparing E2F3 single mutant with the double mutant (Table 2; Supplementary Fig. S1). In other words, this co-occurrence is beneficial for the tumor cell when mutations of *TP53* appear first. We looked more closely at the CIT dataset: There are 58 *TP53*-mutated and 11 *E2F3*-amplified samples in total. We found that among the 11 *E2F3*-amplified tumors, 9 are *TP53*-mutated, and 7 out of these 9 are muscle-invasive. In the Iyer dataset, 15 of 20 *E2F3*-amplified tumors are also *TP53*-mutated. As mentioned in the previous association, amplifying *E2F3* might be one way to favor proliferation when tumors are already *TP53*-mutated.

Co-occurrence of *CCND1* amplifications and *CDKN2A* homozygous deletions has been reported for head and neck squamous cell carcinomas (42, 43) and is found in CIT data. Simulations show that amplifying *CCND1* (CyclinD1 overexpressed) alone has already an advantage over deleting *CDKN2A* (p16INK4a and p14ARF deletions in the model) alone in terms of proliferation (Table 2; Supplementary Fig. S1). It is known that CDKN2A inhibits CCND1 by forming a complex with the CDKs, CDK4 or CDK6. As a consequence, its loss facilitates the activation of CCND1 but does not necessarily promote proliferation. The double mutant shows an increase in proliferation when compared with both single mutants (Table 2; Supplementary Fig. S1). Our model thus confirms co-occurrence of these alterations. The role of *CDKN2A* in senescence is not considered here, and we anticipate that it may play an additional role that we cannot account for in this model.

Co-occurrence of *PIK3CA* mutations and *CDKN2A* homozygous deletions is similar to the previous case. The double mutation increases the probability to reach proliferation compared with single mutants. Indeed, the double mutant PI3K overexpressed and CDKN2A deleted (p16INK4a and p14ARF deletions) suppresses the Growth_arrest attractors (Table 2 and Supplementary Table S6; Supplementary Fig. S1).

Discussion

By performing literature search and data mining of four independent bladder cancer datasets, we identified nine patterns of co-occurrence and mutual exclusivity in genetic alterations affecting growth factor signaling pathways, cell cycle, and apoptosis. To explain the reasons and contexts for these patterns, we defined a mathematical model derived from an influence network encompassing the frequently altered genes (Fig. 4). We simulated the mutants corresponding to the patterns and provided different types of predictions. First, we concluded that, in some cases, co-occurrence needs to be accompanied by a third mutation to be associated with invasiveness, for example, *PIK3CA* mutations or *p21CIP* deletions in an *FGFR3*-mutated and *CDKN2A*-deleted context. Next, we found that the order of mutations might explain associations and concluded that some events occur late during tumorigenesis (e.g., co-occurrence of *TP53* mutations and *E2F3* amplifications).

In some cases, our model suggests that co-occurring genetic alterations prepare a context for more aggressive tumors (e.g., *FGFR3* and *PIK3CA* mutations) or lead to more invasive tumors (e.g., *E2F3* amplifications and *TP53* mutations); and mutually exclusive alterations show redundant effect of the alterations on proliferation probabilities (e.g., *FGFR3* and *RAS* mutations) or may be involved in different tumor types (*FGFR3*-mutated tumors associated to Ta pathway vs. *TP53*-mutated associated to CIS pathway). However, the model shows its limitations when it comes to distinguishing between the two hypotheses for mutual exclusivity. For instance, *FGFR3* mutations and *E2F3* amplifications are found mutually exclusive. In the model, they have the same downstream effect. Thus, we could conclude that one alteration only should be selected or the two alterations belong to different progression pathways as suggested by Lindgren (49). Because of Lindgren's results and the fact that *E2F3* amplifications are co-occurring with *TP53* mutations, we are tempted to associate *E2F3* alterations to CIS progression pathway.

Looking at all nine associations studied with the model (Fig. 3), we can deduce (and confirm) that *FGFR3* and *PIK3CA* mutations along with *CDKN2A* homozygous deletions are more associated with Ta progression pathway, whereas *EGFR*, *E2F3* amplifications, and *TP53* mutations are more associated with CIS progression pathway. *p21CIP* alterations (mutations or loss) seem to be associated with the Ta progression pathway in absence of *PIK3CA* mutations. The assignment of *RAS* mutations to one of the progression pathways was more difficult.

Because cancer is a disease involving multiple alterations and because our model only includes simplified representations of pathways, results from model analysis have to be interpreted with care. Moreover, the model refers to a single, idealized cell, thus ignoring crucial effects from its microenvironment. It would be tempting to suggest that phenotype probabilities predicted by the model for mutation patterns can have improved association to patient survival compared with mutational profile. Cox proportional hazard regression for the model probabilities of the phenotypes (Proliferation, Growth_arrest, Apoptosis) showed a significant association to patient survival. However, the same regression model estimated for the raw mutational profiles gives slightly

more significant results (not shown). It is not yet realistic to expect that our mechanistic model would outcompete statistical approaches in predicting patient survival. This could be explained by the complexity of factors, which affects survival. Our model only focuses on the prediction of cancer cells to become invasive. Nevertheless, this does not compromise the cognitive value of the model to provide mechanistic insights into patterns of gene alterations observed in groups of patients, which is the main focus of the current study.

What the model shows with confidence is that reasoning in terms of pathways is not enough to explain the studied patterns. Linear signaling pathways, as often described in biology, are highly interconnected, and it becomes difficult to reason without a model to formally conclude on the roles of frequent mutations. While the model does not provide straightforward explanations for all associations, or cannot confirm some results of the CIT dataset statistical analysis (see *CCND1* amplifications and *FGFR3* mutations), it allows to explore the effects of single, double, or even triple mutations on the studied phenotypes. For these cases, it can provide qualitative trends (e.g., increase in Proliferation) and lead to the formulation of predictions. The model can propose contexts in which particular mutations lead to extreme cases. For instance, we can interpret proliferative phenotypes, if they are the only reachable stable states, as a very invasive situation in which the cell would have lost all protections against uncontrolled growth (this is the case for the triple mutant FGFR3 overexpressed and PI3K overexpressed and CDKN2A deleted). Our approach combining data analysis and mathematical modeling is able to shed some light on the mechanisms leading to tumorigenesis and allows an alternative interpretation of the genomic data.

Of course, some predictions remain to be checked in other public datasets, as soon as they are made available (e.g., the role of *p21CIP* in invasiveness). To draw our conclusions, we considered copy number and sequencing data, but many other events can happen downstream of gene activity. It would be appropriate to include other types of data, such as mRNA expression, DNA methylation, and protein level. We plan to include at least transcriptomic data in future analyses and anticipate that other genes will appear to play a role in the process of invasiveness.

Finally, we analyzed association patterns limiting ourselves to cell cycle and apoptosis entries. Some of our explanations may be incomplete because of the involvement of important genes in other cell fates such as senescence (e.g., *TP53*, *CDKN2A*, *RBL2*, etc.; ref. 50). Similarly, *PTEN* role will need to be further explored in pathways other than PI3K/AKT as reported in refs. 26, 51.

Disclosure of Potential Conflicts of Interest

No potential conflicts of interest were disclosed.

Authors' Contributions

Conception and design: E. Remy, S. Rebouissou, C. Chaouiya, A. Zinovyev, F. Radvanyi, L. Calzone

Development of methodology: E. Remy, C. Chaouiya, A. Zinovyev, L. Calzone

Acquisition of data (provided animals, acquired and managed patients, provided facilities, etc.): S. Rebouissou, F. Radvanyi

Analysis and interpretation of data (e.g., statistical analysis, biostatistics, computational analysis): E. Remy, S. Rebouissou, C. Chaouiya, F. Radvanyi, L. Calzone

Writing, review, and/or revision of the manuscript: E. Remy, S. Rebouissou, C. Chaouiya, A. Zinovyev, F. Radvanyi, L. Calzone

Administrative, technical, or material support (i.e., reporting or organizing data, constructing databases): E. Remy, L. Calzone

Study supervision: E. Remy, C. Chaouiya, F. Radvanyi, L. Calzone

Acknowledgments

The authors thank Luca Grieco for help in modeling the interaction between EGFR and FGFR3, Gautier Stoll for MaBoSS simulations, Fanny Coffin and Pierre Gestraud for statistical consulting, Anne Biton and Elodie Chapeaublanc for data management/processing, Pedro T. Monteiro for Avatar simulations, and Denis Thieffry and Emmanuel Barillot for critical reading of the manuscript.

Grant Support

This work was supported by Agence Nationale de la Recherche (ANR-08-SYSC-003).

The costs of publication of this article were defrayed in part by the payment of page charges. This article must therefore be hereby marked *advertisement* in accordance with 18 U.S.C. Section 1734 solely to indicate this fact.

Received March 5, 2015; revised June 4, 2015; accepted June 24, 2015; published OnlineFirst August 3, 2015.

References

1. Vogelstein B, Papadopoulos N, Velculescu VE, Zhou S, Diaz LA, Kinzler KW. Cancer genome landscapes. Science 2013;339:1546–58.
2. Yeang C-H, McCormick F, Levine A. Combinatorial patterns of somatic gene mutations in cancer. FASEB J 2008;22:2605–22.
3. Zhang J, Wu L-Y, Zhang X-S, Zhang S. Discovery of co-occurring driver pathways in cancer. BMC Bioinformatics 2014;15:271.
4. Ciriello G, Cerami E, Sander C, Schultz N. Mutual exclusivity analysis identifies oncogenic network modules. Genome Res 2012;22:398–406.
5. Szczurek E, Beerenwinkel N. Modeling mutual exclusivity of cancer mutations. PLoS Comput Biol 2014;10:e1003503.
6. Etemadmoghadam D, Weir BA, Au-Yeung G, Alsop K, Mitchell G, George J, et al. Synthetic lethality between CCNE1 amplification and loss of BRCA1. Proc Natl Acad Sci U S A 2013;110:19489–94.
7. Kreeger PK, Lauffenburger DA. Cancer systems biology: a network modeling perspective. Carcinogenesis 2010;31:2–8.
8. Knudson AG. Mutation and cancer: statistical study of retinoblastoma. Proc Natl Acad Sci U S A 1971;68:820–3.
9. Sahin O, Fröhlich H, Löbke C, Korf U, Burmester S, Majety M, et al. Modeling ERBB receptor-regulated G1/S transition to find novel targets for de novo trastuzumab resistance. BMC Syst Biol 2009;3:1.
10. Saez-Rodriguez J, Alexopoulos LG, Zhang M, Morris MK, Lauffenburger DA, Sorger PK. Comparing signaling networks between normal and transformed hepatocytes using discrete logical models. Cancer Res 2011;71:5400–11.
11. Steinway SN, Gomez Tejeda Zañudo J, Ding W, Rountree CB, Feith DJ, Loughran TP, et al. Network modeling of TGFβ signaling in hepatocellular carcinoma epithelial-to-mesenchymal transition reveals joint Sonic hedgehog and Wnt pathway activation. Cancer Res 2014;74:5963–77.
12. Grieco L, Calzone L, Bernard-Pierrot I, Radvanyi F, Kahn-Perlès B, Thieffry D. Integrative modelling of the influence of MAPK network on cancer cell fate decision. PLoS Comput Biol 2013;9:e1003286.
13. Barillot E, Calzone L, Hupe P, Vert J-P, Zinovyev A. Computational Systems Biology of Cancer. CRC Press; 2012.
14. Kaufman DS, Shipley WU, Feldman AS. Bladder cancer. Lancet 2009;374:239–49.
15. López-Knowles E, Hernández S, Malats N, Kogevinas M, Lloreta J, Carrato A, et al. PIK3CA mutations are an early genetic alteration associated with FGFR3 mutations in superficial papillary bladder tumors. Cancer Res 2006;66:7401–4.

16. Jebar AH, Hurst CD, Tomlinson DC, Johnston C, Taylor CF, Knowles MA. FGFR3 and Ras gene mutations are mutually exclusive genetic events in urothelial cell carcinoma. Oncogene 2005;24:5218–25.
17. Billerey C, Chopin D, Aubriot-Lorton MH, Ricol D, Gil Diez de Medina S, Van Rhijn B, et al. Frequent FGFR3 mutations in papillary non-invasive bladder (pTa) tumors. Am J Pathol 2001;158:1955–9.
18. Spruck CH, Ohneseit PF, Gonzalez-Zulueta M, Esrig D, Miyao N, Tsai YC, et al. Two molecular pathways to transitional cell carcinoma of the bladder. Cancer Res 1994;54:784–8.
19. Neuzillet Y, Paoletti X, Ouerhani S, Mongiat-Artus P, Soliman H, deThe H, et al. A meta-analysis of the relationship between FGFR3 and TP53 mutations in bladder cancer. PLoS One 2012;7:e48993.
20. Cairns P, Tokino K, Eby Y, Sidransky D. Homozygous deletions of 9p21 in primary human bladder tumors detected by comparative multiplex polymerase chain reaction. Cancer Res 1994;54:1422–4.
21. Açikbas I, Keser I, Kiliç S, Bağci H, Karpuzoğlu G, Lüleci G. Detection of LOH of the RB1 gene in bladder cancers by PCR-RFLP. Urol Int 2002;68: 189–92.
22. Knoll S, Fürst K, Kowtharapu B, Schmitz U, Marquardt S, Wolkenhauer O, et al. E2F1 induces miR-224/452 expression to drive EMT through TXNIP downregulation. EMBO Rep 2014;15:1315–29.
23. Schaal C, Pillai S, Chellappan SP. The Rb-E2F transcriptional regulatory pathway in tumor angiogenesis and metastasis. Adv Cancer Res 2014;121: 147–82.
24. Engelmann D, Pützer BM. The dark side of E2F1: in transit beyond apoptosis. Cancer Res 2012;72:571–5.
25. Peña-Llopis S, Christie A, Xie X-J, Brugarolas J. Cooperation and antagonism among cancer genes: the renal cancer paradigm. Cancer Res 2013; 73:4173–9.
26. Calderaro J, Rebouissou S, de Koning L, Masmoudi A, Hérault A, Dubois T, et al. PI3K/AKT pathway activation in bladder carcinogenesis. Int J Cancer 2014;134:1776–84.
27. Sobin LH, Compton CC. TNM seventh edition: what's new, what's changed: communication from the International Union Against Cancer and the American Joint Committee on Cancer. Cancer 2010;116:5336–9.
28. Mostofi FK, Sobin LH, Torloni H. Histological typing of urinary bladder tumours. Tumors WHO: Geneva, Switzerland; 1973.
29. Van Oers JMM, Lurkin I, van Exsel AJA, Nijsen Y, van Rhijn BWG, van der Aa MNM, et al. A simple and fast method for the simultaneous detection of nine fibroblast growth factor receptor 3 mutations in bladder cancer and voided urine. Clin Cancer Res 2005;11:7743–8.
30. Boyault S, Rickman DS, deReyniès A, Balabaud C, Rebouissou S, Jeannot E, et al. Transcriptome classification of HCC is related to gene alterations and to new therapeutic targets. Hepatology 2007;45:42–52.
31. Wallerand H, Bakkar AA, de Medina SGD, Pairon J-C, Yang Y-C, Vordos D, et al. Mutations in TP53, but not FGFR3, in urothelial cell carcinoma of the bladder are influenced by smoking: contribution of exogenous versus endogenous carcinogens. Carcinogenesis 2005;26:177–84.
32. Hupé P, Stransky N, Thiery J-P, Radvanyi F, Barillot E. Analysis of array CGH data: from signal ratio to gain and loss of DNA regions. Bioinformatics 2004;20:3413–22.
33. Rebouissou S, Hérault A, Letouzé E, Neuzillet Y, Laplanche A, Ofualuka K, et al. CDKN2A homozygous deletion is associated with muscle invasion in FGFR3-mutated urothelial bladder carcinoma. J Pathol 2012;227:315–24.
34. Chaouiya C, Naldi A, Thieffry D. Logical modelling of gene regulatory networks with GINsim. Methods Mol Biol 2012;804:463–79.
35. Mendes ND, Monteiro PT, Carneiro J, Remy E, Chaouiya C. Quantification of reachable attractors in asynchronous discrete dynamics. 2014; Available from: http://arxiv.org/abs/1411.3539
36. Stoll G, Viara E, Barillot E, Calzone L. Continuous time Boolean modeling for biological signaling: application of Gillespie algorithm. BMC Syst Biol 2012;6:116.
37. Lindgren D, Frigyesi A, Gudjonsson S, Sjödahl G, Hallden C, Chebil G, et al. Combined gene expression and genomic profiling define two intrinsic molecular subtypes of urothelial carcinoma and gene signatures for molecular grading and outcome. Cancer Res 2010;70:3463–72.
38. Iyer G, Al-Ahmadie H, Schultz N, Hanrahan AJ, Ostrovnaya I, Balar A V, et al. Prevalence and co-occurrence of actionable genomic alterations in high-grade bladder cancer. J Clin Oncol 2013;31:3133–40.
39. The Cancer Genome Atlas Research Network. Comprehensive molecular characterization of urothelial bladder carcinoma. Nature 2014;507:315–22.
40. Juanpere N, Agell L, Lorenzo M, de Muga S, López-Vilaró L, Murillo R, et al. Mutations in FGFR3 and PIK3CA, singly or combined with RAS and AKT1, are associated with AKT but not with MAPK pathway activation in urothelial bladder cancer. Hum Pathol 2012;43:1573–82.
41. Hurst CD, Tomlinson DC, Williams S V, Platt FM, Knowles MA. Inactivation of the Rb pathway and overexpression of both isoforms of E2F3 are obligate events in bladder tumours with 6p22 amplification. Oncogene 2008;27:2716–27.
42. Bova RJ, Quinn DI, Nankervis JS, Cole IE, Sheridan BF, Jensen MJ, et al. Cyclin D1 and p16INK4A expression predict reduced survival in carcinoma of the anterior tongue. Clin Cancer Res 1999;5:2810–9.
43. Rothenberg SM, Ellisen LW. The molecular pathogenesis of head and neck squamous cell carcinoma. J Clin Invest 2012;122:1951–7.
44. Calzone L, Gelay A, Zinovyev A, Radvanyi F, Barillot E. A comprehensive modular map of molecular interactions in RB/E2F pathway. Mol Syst Biol 2008;4:173.
45. Croft D, Mundo AF, Haw R, Milacic M, Weiser J, Wu G, et al. The Reactome pathway knowledgebase. Nucleic Acids Res 2014;42:D472–7.
46. Laé M, Couturier J, Oudard S, Radvanyi F, Beuzeboc P, Vieillefond A. Assessing HER2 gene amplification as a potential target for therapy in invasive urothelial bladder cancer with a standardized methodology: results in 1005 patients. Ann Oncol 2010;21:815–9.
47. Korkolopoulou P, Konstantinidou AE, Thomas-Tsagli E, Christodoulou P, Kapralos P, Davaris P. WAF1/p21 protein expression is an independent prognostic indicator in superficial and invasive bladder cancer. Appl Immunohistochem Mol Morphol 2000;8:285–92.
48. Rebouissou S, Bernard-Pierrot I, de Reyniès A, Lepage M-L, Krucker C, Chapeaublanc E, et al. EGFR as a potential therapeutic target for a subset of muscle-invasive bladder cancers presenting a basal-like phenotype. Sci Transl Med 2014;6:244–91.
49. Lindgren D, Sjödahl G, Lauss M, Staaf J, Chebil G, Lövgren K, et al. Integrated genomic and gene expression profiling identifies two major genomic circuits in urothelial carcinoma. PLoS ONE 2012;7:e38863.
50. Fiorentino FP, Symonds CE, Macaluso M, Giordano A. Senescence and p130/Rbl2: a new beginning to the end. Cell Res 2009;19:1044–51.
51. Seront E, Pinto A, Bouzin C, Bertrand L, Machiels J-P, Feron O. PTEN deficiency is associated with reduced sensitivity to mTOR inhibitor in human bladder cancer through the unhampered feedback loop driving PI3K/Akt activation. Br J Cancer 2013;109:1586–92.
52. Cosmic data: http://cancer.sanger.ac.uk/cancergenome/projects/cosmic/
53. Atlas of Cancer Signalling Network: http://acsn.curie.fr/.